Adipocyte-Derived Amino Acid Storage Proteins are Required for Germline Stem Cell Maintenance in Adult *Drosophila* Females

Anna B. Zike[1], Mekenzi O. Hazen[1], Madison G. Abel[1], Eleanor B. Goldstone[1] Robert C. Eisman[1], and Lesley N. Weaver[1]*

[1]Department of Biology, Indiana University, Bloomington, IN 47405, USA.

Running title: Storage protein regulation of ovarian stem cells

***Corresponding author. Email: lnweaver@iu.edu**

ABSTRACT

Tissue homeostasis is dependent on precise coordination between endocrine organs in response to changes in organism physiology. Secreted circulating factors from adipocytes regulate the behavior of stem cell lineages in peripheral tissues in multiple organisms. In addition to their endocrine roles, *Drosophila* adipocytes store and secrete amino acid storage proteins throughout development. During the larval feeding period, adipocytes secrete storage proteins into the hemolymph, which are reabsorbed by the adipose tissue during metamorphosis to control adult organ size and fertility. Despite the known functions for storage proteins during the larval stages, their requirement during *Drosophila* adulthood and reproduction are uncharacterized. We discover that adipocyte-specific knockdown of the storage proteins *Larval serum protein 1* (*Lsp1*) $\alpha/\beta/\gamma$ and *Larval serum protein 2* (*Lsp2*) results in a decrease in GSC maintenance. We further reveal that decreased GSC number is due to downregulation of Target of Rapamycin (TOR) signaling in GSCs, suggesting compromised amino acid sensing directly in GSCs. We also find that the proteins that mediate storage protein adipocyte reabsorption, Fat body protein 1 (Fbp1) and Fat body protein 2 (Fbp2), are expressed in ovarian follicle cells. Intriguingly, Fbp1 nor Fbp2 appear to be required in follicle cells for GSC maintenance, suggesting undiscovered requirements for amino acid storage proteins in oogenesis. Our results highlight a novel role for *Drosophila* amino acid storage proteins during adulthood and in regulating tissue stem cell lineages.

KEYWORDS: Oogenesis, Fbp1, Fbp2, Lsp1, Lsp2

INTRODUCTION

Multicellular organisms rely on precise coordination of circulating factors between organs to regulate developmental processes and maintain tissue homeostasis during adulthood (Castillo-Armengol et al., 2019; Droujinine and Perrimon, 2016; Katagiri, 2023), and defects in interorgan communication can result in tissue dysfunction and disease (Alvarez-Ochoa et al., 2021). For example, fasting-induced intestinal secretion of the insulin peptide (INS-7) coordinates the gut-to-brain axis to control fat mobilization in *C. elegans* (Liu et al., 2024). Intermittent fasting in mammals activates adrenal glands to stimulate the release of free fatty acids in the hair follicle stem cell (HFSC) niche, resulting in increased levels of reactive oxygen species to induce HFSC death (Chen et al., 2025). Therefore, understanding the unique mechanisms used by different organs to communicate their physiological state can provide insight to how stem cell lineages and tissue homeostasis are maintained during adulthood.

The adult *Drosophila* ovary is an ideal model to understand interorgan control of stem cell lineages due to the conservation of signaling pathways (Hales et al., 2015; Mohr, 2018) and the unparalleled genetic toolkit that allows genetic manipulation of distinct cell types (Roote and Prokop, 2013). Each female contains two ovaries that are arranged in repeating units of 16-20 ovarioles (**Fig. 1A**) with continuously developing egg chambers. Continuous follicle production is dependent on the germline stem cell (GSC) population located in the anterior germarium (**Fig. 1B**). Each germarium houses two-to-three GSCs that divide asymmetrically to produce a self-renewing GSC and differentiating stem cell progeny (Drummond-Barbosa, 2019). Oogenesis is energetically intensive, and GSCs are sensitive to nutrient changes (Drummond-Barbosa, 2019; Drummond-Barbosa and Spradling, 2001). For example, a protein poor diet reduces GSC maintenance and results in death of differentiating progeny (Drummond-Barbosa and Spradling, 2001; Hsu and Drummond-Barbosa, 2009). Furthermore, brain-derived *Drosophila* insulin-like peptides directly regulate GSC division (LaFever and Drummond-Barbosa, 2005) and GSCs directly sense amino acids to activate Target of Rapamycin (TOR) signaling to influence GSC

75 self-renewal and proliferation (LaFever et al., 2010). These studies suggests that complex
76 coordination between organism physiology, organ homeostasis, and control of stem cell
77 lineages is highly regulated in *Drosophila* females.

78 The adipose tissue (also known as the “fat body” in *Drosophila*) is a major site of fat
79 storage and carbohydrate metabolism and has significant endocrine functions to mediate
80 interorgan homeostasis through regulated secretion of adipokines (Morigny et al., 2021; Sakers
81 et al., 2022). The fat body is composed of adipocytes and hepatocyte-like oenocytes, making it
82 similar to the mammalian adipose and liver tissue (Arrese and Soulages, 2010; Chatterjee and
83 Perrimon, 2021; Li et al., 2019). In *Drosophila*, adipocyte-specific metabolic activity impacts
84 GSC maintenance. For example, loss of fatty acid beta oxidation, iron transport, and amino acid
85 transport in adipocytes have been shown to decrease GSC number (Matsuoka et al., 2017).
86 Furthermore, we previously demonstrated that signaling downstream of the nuclear receptor
87 Seven up (Svp) in adipocytes is required to maintain GSC number and prevent death of
88 differentiating stem cell progeny (Weaver and Drummond-Barbosa, 2019). However, the precise
89 signaling mechanisms from adipocytes to GSCs have not been fully elucidated.

90 In addition to lipids and fats, insect adipose tissue stores proteins in the form of amino
91 acid storage proteins (hereafter referred to as “storage proteins”) (Haunerland, 1996; Telfer and
92 Kunkel, 1991). Storage proteins are hexamerins composed of six identical or similar subunits
93 that range in molecular weight from 70 to 90 kDa each (Telfer and Kunkel, 1991). Storage
94 proteins are enriched for methionine or aromatic amino acids (phenylalanine, tryptophan, and
95 tyrosine) and show a high degree of sequence similarity to arthropod hemanocyins (Telfer and
96 Kunkel, 1991). In *Drosophila*, storage proteins have been extensively studied during the larval
97 stages and metamorphosis. The *Drosophila* genome contains four storage proteins, which
98 include the homohexamer, Larval serum protein 2 (Lsp2), and the heterohexamer composed of
99 Larval serum protein 1α (Lsp1α), Lsp1β, and Lsp1γ. During the larval feeding period Lsp1α/β/γ
100 and Lsp2 are synthesized by and secreted from the fat body (Burmester and Scheller, 1997;

101 Roberts et al., 1977). The proteins encoded by *Fat body protein 1* (*Fbp1*) and *Fat body protein 2*
102 (*Fbp2*) are the predicted receptors for LSPs (Akam et al., 1978; Wolfe et al., 1977). LSPs are
103 reabsorbed by adipocytes during metamorphosis in a Fbp1-dependent manner, where they are
104 utilized to control adult organ size and fitness (Valzania et al., 2024). However, Fbp1 and Fbp2
105 lack transmembrane domains and are found in the hemolymph (Valzania et al., 2024),
106 suggesting an unidentified receptor may also influence storage protein reabsorption in
107 adipocytes.

108 Storage proteins have also been observed in adult *Drosophila*. Larval serum protein 2
109 (Lsp2) was previously shown to be synthesized in the adult *Drosophila* fat body (Benes et al.,
110 1990). While no clear role has been defined for storage proteins in adult *Drosophila*, protein
111 levels of LSPs, Fbp1, and Fbp2 in adult female adipocytes have been shown to be sensitive to
112 dietary changes (Matsuoka et al., 2017) and we previously reported that storage protein
113 transcript levels are positively regulated by Svp (Weaver and Drummond-Barbosa, 2020).
114 Furthermore, homozygous *Drosophila Lsp1* mutants are infertile, suggesting undiscovered
115 mechanisms for storage protein regulation of fertility in *Drosophila* (Roberts et al., 1991). These
116 studies suggest that storage proteins may have roles in adult *Drosophila* to regulate tissue
117 homeostasis and reproduction.

118 In this study we investigated the role of storage proteins in the regulation of the adult
119 female *Drosophila* GSC lineage. Using tissue-specific manipulations, we found that adipocyte-
120 derived storage proteins are required to regulate GSC maintenance. We found that adipocyte-
121 derived Lsp1 and Lsp2 are required for activation of TOR signaling in GSCs for their
122 maintenance. We also generated a suite of CRISPR knock-in fusion lines and demonstrate that
123 storage proteins are expressed during adulthood and are also produced in the adult female
124 ovarian follicle cells. We also present intriguing results that although Fbp1 is required for
125 storage protein uptake in larval adipocytes, knockdown of *Fbp1* in adult female adipocytes does
126 not influence GSC number. These results suggest a role for a yet-to-be identified intermediary

127 processor of adipocyte-derived LSPs in maintaining GSCs. Together, our results highlight a
128 previously unknown role for adipocyte-derived storage proteins during adulthood in the
129 regulation of oogenesis.
130

131 **MATERIALS AND METHODS**

132 ***Drosophila strains and culture***

133 *Drosophila* stocks were maintained on Bloomington *Drosophila* Stock Center (BDSC)
134 Cornmeal Food that consists of 15.9 g/L inactive yeast, 9.2 g/L soy flour, 67 g/L yellow
135 cornmeal, 5.3 g/L agar, 70.6 g/L light corn syrup, 0.059 M propionic acid at 22-25°C. Medium
136 was supplemented with active wet yeast paste for all experiments. Flies were kept at a 12 hr/12
137 hr light/dark cycle at all temperatures unless otherwise noted. Previously described *Gal4* and
138 *Gal80* transgenes were used, including *3.1Lsp2-Gal4* (Armstrong et al., 2014; Lazareva et al.,
139 2007), *Cg-Gal4* (Asha et al., 2003), and *tubGal80*^{ts} (McGuire et al., 2003). *UAS-Luc*^{JF01355}
140 (Matsuoka et al., 2017), *UAS-Fbp2*^{GLC01665} (Ni et al., 2011) (Transgenic RNAi Project;
141 fgr.hms.harvard.edu/), *mTOR*$^{\Delta P}$ (Zhang et al., 2000), *Thor*^{2} (Bernal and Kimbrell, 2000), *UAS-*
142 *nucGFP*, *UAS-2xEGFP*, *y*^{1}*w*^{1}, and *Oregon-R* were obtained from the Bloomington *Drosophila*
143 Stock Center (BDSC; bdsc.indiana.edu/). *UAS-Fbp1*^{GD5143}, *UAS-Lsp1*$\alpha^{KK106904}$, *Lsp1*$\beta^{GD12786}$,
144 *UAS-Lsp1*γ^{GD5358}, *UAS-Lsp2*^{GD6088}, and *UAS-Lsp2*^{KK115182} were obtained from the Vienna
145 *Drosophila* RNAi Stock Center (VDRC; https://shop.vbc.ac.at/vdrc_store/). Lines carrying
146 multiple genetic elements were generated by standard crosses. Balancer chromosomes and
147 other genetic elements are described on Flybase (www.flybase.org/).
148

149 ***Generation of CRISPR Knock-In GFP-tagged transgenes***

150 Briefly, gRNA donors were designed to knock in eGFP at the C-terminal end of each
151 protein. Transgenesis was performed using either *yw; nosCas9 attp40* or *yw; nosCas9attp2*.

152 CRISPR knock-in eGFP transgenic lines were designed, microinjected, and balanced by
153 Rainbow Transgenic Fly, Inc (Camarillo, CA). Positive eGFP transgenic lines were verified by
154 screening for eGFP fluorescence intensity and western blot analysis.
155
156 **Western blot analysis in whole larvae and adult females**
157 For western blot analysis, 10 mid-to-late 3rd instar larvae, 10 whole females, 40
158 carcasses, or 40 pairs of ovaries from five-day old wet yeast fed females were collected and
159 flash frozen in liquid nitrogen. Samples were homogenized on dry ice by hand using a tissue
160 grinder, and 200 µl of lysis buffer [1X RIPA buffer (Fisher Scientific), 1X Halt Protease Inhibitor
161 Cocktail (Fisher Scientific)] was added. Samples were incubated on ice for 10 minutes and
162 centrifuged at 13,000 RPM at 4°C for 15 minutes. 150 µl of supernatant was added to 40 µl of
163 4X NuPAGE LDS Sample Buffer (1X, Invitrogen) plus 4% β-mercaptoethanol (Sigma Aldrich)
164 and samples were boiled at 70°C for 10 minutes. Protein concentration was determined using
165 the Pierce BCA Protein Assay Kit (Thermo Scientific) according to manufacturer instructions.
166 30 µg of total protein from each sample was loaded on a 7.5% SDS-polyacrylamide gel
167 and transferred to nitrocellulose. Total protein was stained by incubating membranes in
168 Ponceau (Thermo Scientific) followed by three 5-minute washes with TBST. Blots were blocked
169 in blocking buffer [20 mM Tris pH 7.5, 150 mM NaCl (TBS), 0.1% Tween 20 (TBST), and 5%
170 nonfat dry milk] and probed with polyclonal rabbit anti-GFP (gift from Claire Walczak, 0.25 – 1.9
171 µg/ml) diluted in Abdil-T (TBST, 2% BSA, and 0.1% sodium azide). Membranes were incubated
172 overnight at 4°C, washed in TBST followed by donkey anti-rabbit IgG HRP-linked secondary
173 antibody (1:5000 – 1:40,000) for 1 hour, washed in TBST, and detected with Clarity Western
174 ECL Substrate Working Reagent (Bio-Rad) according to manufacturer's instructions.
175

176 **Larval adipocyte-specific RNAi interference (RNAi)**

177 For knockdown of eGFP-tagged storage proteins in adipocytes, 3rd instar larvae carrying
178 the *UAS-hairpin* of interest (against *Fbp1*, *Lsp1g*, or *Lsp2*) in combination with *Cg-Gal4/CyO*;
179 *storage protein::eGFP/TM6B* (or in the case for Fbp2::eGFP, the eGFP-tagged protein was
180 combined with the *Fbp2 RNAi* transgene and crossed with *Cg-Gal4*) were raised at 29°C to
181 induce transgene expression during development. Amino acid storage protein knockdown
182 larvae and their sibling controls were flash frozen and harvested for western blot analysis as
183 described above.

184

185 **Adult tissue-specific analyses**

186 Females containing the *UAS-transgene* of interest (*2xEGFP*, *nucGFP*, *Luc RNAi*, *Fbp1*
187 *RNAi*, *Fbp2 RNAi*, *Lsp1α RNAi*, *Lsp1β RNAi*, or *Lsp2 RNAi*) in combination with *y w;*
188 *tubGal80^{ts}/CyO; 3.1Lsp2-Gal4/TM3*, *y w; Thor^{2}/CyO; 3.1Lsp2-Gal4 tubGal80^{ts}*, *mTOR$^{\Delta P}$/CyO;*
189 *3.1Lsp2-Gal4 tubGal80^{ts}*, *y w; tj-Gal4 tubGal80^{ts}/CyO*, or *y w; tj-Gal4 tubGal80^{ts}/CyO; nSyb-*
190 *Gal80/TM6B* were raised at 18°C to block Gal4 activity (and therefore, transgene expression)
191 during development. Zero-to-2-day-old females (with *Oregon-R* males) were kept at 18°C for 2-3
192 days and subsequently switched to 29°C. *UAS-Luc^{JF01355}* was used as an RNAi control. As
193 additional controls, females of similar genotypes but without *Gal4/Gal80^{ts}* (*UAS*-alone controls)
194 were raised and maintained under similar conditions for 5-15 days after switching to 29°C. For
195 all conditions, medium was supplemented with wet active yeast paste.

196

197 **Tissue immunostaining and fluorescence microscopy**

198 Ovaries and other tissues were dissected in unsupplemented Grace's Insect Medium
199 (Gibco), fixed, and washed as described (Weaver and Drummond-Barbosa, 2019). Samples
200 were blocked for at least 3 hours at room temperature in 5% normal goat serum (NGS; MP

201 Biomedicals) plus 5% bovine serum albumin (BSA, Sigma Aldrich) in phosphate-buffered saline
202 (PBS; 10 mM NaH_2PO_4/$NaHPO_4$, 175 mM NaCl, pH 7.4) containing 0.1% Triton X-100 (PBST),
203 and incubated overnight at 4°C in primary antibodies diluted in blocking solution as follows:
204 mouse monoclonal anti-α-Spectrin (3A9) (DSHB; Developmental Studies Hybridoma Bank, 3
205 µg/ml); mouse monoclonal anti-Lamin C (LC28.26) (DSHB, 0.8 µg/ml); rat monoclonal anti-E-
206 Cadherin concentrate (DCAD2-c) (DSHB, 0.37 µg/ml); rabbit monoclonal anti-p4E-BP1
207 (Thr37/46) (Cell Signaling Technology, 1 µg/ml), rabbit polyclonal anti-GFP (Fisher Scientific, 1
208 µg/ml), chicken polyclonal anti-GFP (Abcam), and rabbit polyclonal anti-Vasa (Boster Bio, 1
209 µg/ml). Samples were washed in PBST and incubated for 2 hours at room temperature in 1:200
210 Alexa Fluor 488- or 568-conjugated goat species-specific secondary antibodies (Invitrogen) in
211 blocking solution. Stained samples were washed, mounted in Vectashield containing 1.5 µg/ml
212 4',6-diamidino-2-phenylindole (DAPI) (Vector Laboratories), and imaged using a Nikon SP8
213 confocal microscope.
214 GSCs and cap cells were identified as described (Weaver and Drummond-Barbosa,
215 2019), and two-way ANOVA with interaction (GraphPad Prism) was used to calculate the
216 statistical significance of any differences among genotypes in the rate of cap cell or GSC loss
217 from at least three independent experiments, as described (Armstrong et al., 2014).
218 For Dad::nlsGFP quantification, the densitometric mean of individual GSC nuclei was
219 measured from optical sections containing the largest nuclear diameter (visualized by DAPI)
220 using FIJI (https://fiji.sc/) (Armstrong et al., 2014). For E-Cadherin quantification, the total
221 densitometric value from maximum intensity projections around the cap cells (identified using
222 LamC staining) was measured with FIJI (Weaver and Drummond-Barbosa, 2018).
223 Quantification of E-Cadherin levels by immunofluorescence is a well-established method to
224 determine whether adherence of GSCs to the niche is compromised (Hsu and Drummond-
225 Barbosa, 2011). p4E-BP1 levels were determined by taking Z-stacks through the whole GSC

226 and total stack intensity was projected. Densitometric data for Dad::nlsGFP, E-Cadherin, and
227 p4E-BP1 levels were subjected to the Mann-Whitney *U*-test.
228 For lipid droplet visualization, fixed and washed fat bodies attached to abdominal
229 carcasses were incubated with 2.5X Alexa Fluor 488-conjugated phalloidin (Molecular Probes)
230 in PBST for 20 min, rinsed, and washed three times for 15 min each in PBST. Abdominal
231 carcasses were incubated in 25 ng/ml Nile Red dye for 10 min. Samples were stored in
232 Vectashield plus DAPI (Vector Laboratories) and fat bodies were scraped off the abdominal
233 carcass and imaged using a Nikon SP8 confocal. The largest cell area of each adipocyte (based
234 on phalloidin staining) used to measure adipocyte area; whereas the longest width of each
235 nucleus per adipocyte (based on DAPI) determined nuclear diameter. Each measurement was
236 performed using FIJI. Three independent experiments were performed, and statistical analysis
237 was performed using a Student's *t* test.
238 For analysis of eGFP-tagged amino acid storage protein localization in female
239 adipocytes, larval fat bodies were fixed in 5.3% formaldehyde in Grace's media for 13 min (20
240 min for adult female fat) at room temperature. Samples were subsequently rinsed and washed
241 three times for 15 min each in 1X PBS containing 0.5% Tween. Samples were blocked for at
242 least 3 hours in block solution containing 1X PBS, 0.5% Tween, 5% NGS, and 5% BSA.
243 Samples were incubated in polyclonal rabbit anti-GFP (Fisher Scientific, 1 µg/ml) at 4 degrees
244 overnight. Fat bodies were washed in PBS-0.5% Tween and incubated for 2 hours at room
245 temperature in 1:200 Alexa Fluor 488-conjugated goat anti-rabbit secondary antibody
246 (Invitrogen) in blocking solution. Samples were subsequently incubated in 2.5X Alexa-594
247 phalloidin (Molecular Probes) in PBS-0.5% Tween for 20 min, rinsed, and washed three times
248 for 15 min each in PBS-0.5% Tween. Stained samples were washed, mounted in Vectashield
249 containing 1.5 µg/ml 4',6-diamidino-2-phenylindole (DAPI) (Vector Laboratories). Images were
250 collected on a Nikon SP8 confocal microscope at 0.5 µm intervals, and 3-5 z-planes were
251 combined for analysis. For adult fat eGFP analysis, puncta from at least 25 adipocytes were

252 measured from at least four independent experiments, and statistical analysis was performed
253 using a paired Student's *t* test.
254
255 **ApopTag Assays**
256 To detect dying germline cysts, the ApopTag Indirect *In Situ* Apoptosis Detection Kit (Millipore
257 Sigma) was used according to the manufacturer's instructions as previously described (Weaver
258 and Drummond-Barbosa, 2019). Briefly, fixed and teased ovaries were rinsed in equilibration
259 buffer twice for 5 minutes each at room temperature. Samples were incubated in 100 µl TdT
260 solution at 37°C for 1 hour with mixing at 15-minute intervals. Ovaries were washed three times
261 in 1X PBS followed by incubation in anti-digoxigenin conjugate for 30 min at room temperature
262 protected from light. Samples were washed four times in 1X PBS and processed for
263 immunofluorescence as described above.
264
265 **RNA isolation**
266 Abdominal carcasses from 100 females of each genotype were dissected in Grace's
267 medium supplemented with 10% fetal bovine serum (FBS; Sigma) as previously described
268 (Weaver and Drummond-Barbosa, 2020). Fat body cells were dissociated from abdominal
269 carcasses with 500 µl dissociation buffer [0.2% Trypsin (Sigma) plus 2 mg/ml collagenase
270 (Sigma) in 1x PBS] per 50 carcasses for 30 minutes at room temperature. Samples were gently
271 agitated every 5 minutes to facilitate separation of cells from the cuticle. 500 µl of Grace's media
272 plus 10% FBS was added to stop the enzymatic reaction, and supernatants were placed in new
273 tubes. Carcasses were rinsed with Grace's medium plus 10% FBS and the two supernatants
274 per genotype were combined. Dissociated cells were centrifuged at 3.3 rpm for 5 min at room
275 temperature. Supernatants were removed and cells were flash frozen in liquid nitrogen. Cells
276 were lysed in 250 µl lysis buffer from the RNAqueous-4PCR DNA-free RNA isolation for RT-
277 PCR kit (Ambion). RNA was extracted from all samples following the manufacturer's

278 instructions. Three independent experiments were performed for quantitative reverse-
279 transcriptase polymerase chain reaction (qRT-PCR) analysis.
280
281 **cDNA synthesis and quantitative reverse-transcriptase polymerase chain reaction (qRT-**
282 **PCR)**
283 cDNA was synthesized from 500 ng of total RNA described above for each sample using
284 Superscript II Reverse Transcriptase (Thermo Fisher Scientific) according to the manufacturer's
285 instructions. PowerUp SYBR Green Master Mix (Thermo Fisher Scientific) was used for RT-
286 qPCR. The reactions for three independent biological replicates were performed in triplicate
287 using LightCycler 96 (Roche). Amplification fluorescence threshold was determined by
288 LightCycler 96 software, and ddCT were calculated using Microsoft Excel. Fold change of
289 transcript levels was calculated in Excel as described (Taylor et al., 2019). The primers used for
290 all PCR reactions are listed in Table S1. *Rp49* and *Act5C* transcript levels were used as
291 references.
292
293 **Survival assays**
294 For survival analysis, four-to-six vials containing 25 two-to-four-day old, mated females
295 were incubated at 29ºC. Vials were flipped every 1–3 days until no living flies remained in the
296 vials. Death was recorded when the flies were flipped to fresh food. Data was plotted in
297 GraphPad Prism (GraphPad) and survival curve statistical analysis was performed using a log-
298 rank test.
299
300 **Egg count assays**
301 Egg count analysis was performed as previously described (Weaver and Drummond-
302 Barbosa, 2019). Briefly, five females of the appropriate genotype and five y^1 w^1 males were
303 maintained at 29ºC in perforated plastic bottles capped with molasses/agar plates

304 supplemented with active yeast paste. Plates were changed twice daily, and the number of eggs
305 per day was counted in five replicates per genotype. Data was subjected to a paired Student's *t*-
306 test.
307
308 **Fly Liquid-Food Interaction Counter (FLIC) assay**
309 The Fly Liquid-Food Interaction Counter (FLIC) system was used to determine
310 differences in feeding behavior as previously described (Fleck et al., 2024; Ro et al., 2014).
311 FLIC *Drosophila* Feeding Monitors (DFMs, Sable Systems International, models DFMV2 and
312 DFMV3) were used in the single choice configuration and each chamber was loaded with liquid
313 food solution [4% sucrose (m/v), 1.5% yeast extract (m/v)]. Females incubated at 29ºC for 10
314 days were switched from solid food to liquid food at 29ºC overnight (~8-12 hours) prior to
315 running each experiment. Flies were aspirated into the DFM chambers and feeding behavior
316 was measured for 24 hours. Each FLIC experiment contains pooled data from at least 30 flies
317 for each genotype. FLIC data were analyzed using previously described custom R code (Ro et
318 al., 2014), which is available at https://github.com/PletcherLab/FLIC_R_Code. Default
319 thresholds were used for analysis except for the following: minimum feeding threshold = 10,
320 tasting threshold = (0,10). Animals that did not participate (i.e., returned zero values), whose
321 DFM returned an unstable baseline signal, or who produced extreme outliers (i.e., exceeding
322 twice the mean of the population) were excluded from analysis. Data were subjected to a Mann-
323 Whitney *U*-test.
324
325 **RESULTS**
326 ***Adipocyte-derived amino acid storage proteins are required for GSC maintenance.***
327 Storage proteins are required for fecundity in many adult insects; however, the
328 requirement for storage proteins during oogenesis in *Drosophila* has been understudied. We
329 previously performed transcriptomics on the adult female fat body to identify signaling

330 components downstream of Svp. Analysis of this data revealed that *Lsp1α/β*, *Lsp2*, and *Fbp2*
331 transcripts were significantly downregulated in females where *svp* was depleted from the fat
332 body (**Fig. 1C**; (Weaver and Drummond-Barbosa, 2020); however, it is unknown whether LSPs
333 or Fbp2 are direct targets of Svp from this dataset. Furthermore, adipocyte-specific affinity
334 labeling of secreted peptides identified storage proteins in adult hemolymph (Droujinine et al.,
335 2021), and a previous proteomics analysis determined that storage proteins are sensitive to
336 changes in diet in adult female adipocytes [**Fig. 1D**; (Matsuoka et al., 2017)]. We therefore
337 decided to test the involvement of adipocyte-derived storage proteins in regulating the GSC
338 lineage.
339 To assess whether storage proteins are expressed in adult females, we utilized a
340 CRISPR knock-in strategy to express enhanced GFP (eGFP) at the C-terminal end of the
341 endogenous protein (Lsp1γ and Lsp2) and analyzed protein expression in female larval and
342 adult adipocytes by western blot analysis (**Fig. 1E and F; Fig. S1A and B**). To test the
343 specificity of our eGFP knock-in lines, we knocked down *Lsp1γ* and *Lsp2* in larval adipocytes
344 during development using the *Cg-Gal4* driver (Asha et al., 2003) and observed a significant
345 decrease in eGFP-tagged protein levels relative to controls (**Fig. S1A and B**). We next analyzed
346 the expression pattern in adipocytes by immunofluorescence using *Oregon-R* as a negative
347 control (**Fig. 1G and H**). In larval female adipocytes, Lsp1γ::eGFP (representing the
348 heterohexameric complex of Lsp1α/β/γ) and Lsp2::eGFP are abundantly expressed (**Fig. 1G**)
349 and form granule-like structures in the cytosol. In contrast, storage protein expression in adult
350 female adipocytes is significantly decreased compared to larval female adipocytes (**Fig. 1H**),
351 showing small Lsp1γ::eGFP and Lsp2::eGFP puncta (**Fig. 1I)**. Collectively, these results
352 suggest that although storage proteins are not as highly expressed in the adipocytes of adult
353 females compared to larvae, they are detected and may have functional roles during adulthood.
354

355 ***Adipocyte-derived amino acid storage proteins are required for GSC maintenance.***

356 We next asked whether adipocyte-secreted Lsp1α/β/γ and Lsp2 are required for early
357 processes of oogenesis (GSC maintenance or survival of early germline cysts). Individual
358 knockdown of *Lsp1α* or *Lsp1β* is sufficient to decrease the transcript levels of all components of
359 the Lsp1 complex (**Fig. S2A, B, and D**; (Valzania et al., 2024). Therefore, we knocked down
360 *Lsp1α*, *Lsp1β*, or *Lsp2* (**Fig. S2C and E**) specifically in adult adipocytes using the previously
361 described *tubGal80^{ts}; 3.1Lsp2-Gal4* (*3.1Lsp2^{ts}*) driver (Armstrong et al., 2014) and assayed
362 GSC number over 15 days by staining ovaries with α-Spectrin to label GSCs and Laminin C to
363 label cap cell nuclear lamina (**Fig. 2A and B**). Knockdown of *Lsp1α/β* and *Lsp2* in adult female
364 adipocytes significantly increased the rate of GSC loss compared to *Luc* control (**Fig. 2C and D;**
365 **Fig. S2F and G**). The loss of GSCs was not due to leaky expression of the *UAS* transgenes, as
366 there was no significant decrease in GSC number of *UAS-alone* controls over time compared to
367 the *UAS-Luc* RNAi hairpin (**Fig. S2H and I**). In addition, the decrease in GSC maintenance was
368 not dependent on the size of the niche (Hsu and Drummond-Barbosa, 2009), as cap cell
369 numbers were unaffected (**Fig. S2J and K**). Furthermore, GSC loss was not due to gross
370 disruption of adipose tissue as measured by adipocyte nuclear or cell size (**Fig. S3**).

371 It was recently shown that dietary restriction due to reduction of *Lsp2* in larvae increases
372 lifespan during adulthood (Kosakamoto et al., 2025). Consistent this, we also observed a slight,
373 but significant lifespan enhancement when *Lsp1a* or *Lsp2* were knocked down specifically in
374 adult adipocytes (**Fig. S4A and B**), suggesting that dietary restriction (via lower storage protein
375 levels) may enhance lifespan at the expense of reproductive fitness. We also explored whether
376 loss of LSPs in adipocytes altered feeding behavior using the Fly Liquid food Interaction
377 Counter (FLIC) and did not observe any change in the number of feeding events or duration of
378 feeding compared to *Luc* RNAi control (**Fig. S4C-F**).

379 Notably, storage protein knockdown did not influence the number of eggs laid by
380 females compared to *Luc* control over a two-week period (**Fig. S4G**). It should be noted,
381 however, that egg count analyses do not always reveal subtle changes in oogenesis (Ma et al.,
382 2020; Weaver and Drummond-Barbosa, 2019), especially defects occurring at early stages in
383 the germline. Production of a mature oocyte from a GSC takes approximately seven days (He et
384 al., 2011) and changes in GSC maintenance due to adipocyte-specific storage protein
385 knockdown are not observed until 10 days after transgene expression; therefore, it is unlikely
386 that changes in egg production would be observed by 15 days. Furthermore, egg production is
387 significantly inhibited at higher temperatures in wild-type strains (Gandara and Drummond-
388 Barbosa, 2022), preventing long-term observation of consequences from GSC maintenance
389 defects. Our data suggest that although loss of *Lsp1a* and *Lsp2* enhances adult female lifespan,
390 additional physiological effects that could influence GSC maintenance were unaffected.
391 To assess whether knockdown of *Lsp1α/β/γ* or *Lsp2* influences survival of early germline
392 cysts, we labeled germaria with ApopTag, which is a TUNEL-based assay to detect significant
393 DNA fragmentation that is indicative of apoptosis (Drummond-Barbosa and Spradling, 2001).
394 Compared to *Luc* control, knockdown of *Lsp1α/β/γ* or *Lsp2* in adipocytes did not significantly
395 increase the percentage of ApopTag positive germline cysts 10 days after transgene expression
396 (**Fig. S5**). Collectively, these results suggest that Lsp1α/β/γ and Lsp2 are required in adult
397 female adipocytes to control GSC maintenance.
398
399 ***Storage protein reabsorption by Fbp1 or Fbp2 does not regulate GSC maintenance.***
400 Reabsorption of storage proteins in adipocytes during pupariation is dependent on Fbp1
401 (Valzania et al., 2024). Considering Fbp1 and Fbp2 proteins are present in adult female fat and
402 are also regulated by a protein-rich diet, we hypothesized that Fbp1-mediated retrieval of
403 storage proteins may promote GSC self-renewal. We assessed Fbp1 and Fbp2 expression in

404 adult female adipocytes using our eGFP CRISPR knock-in constructs, which were confirmed to
405 be specific based on western blot analysis of knockdown of *Fbp1* or *Fbp2* in the larval fat body
406 compared to control (**Fig. S1C and D**).
407 Immunofluorescence analysis showed that Fbp1::eGFP is expressed in granules in
408 female larvae adipocytes, however Fbp2::eGFP has a more diffuse expression pattern (**Fig.**
409 **3A**). In contrast, Fbp1 and Fbp2 expression in adult female adipocytes is decreased and shows
410 variable puncta levels compared to the *Oregon-R* control (**Fig. 3B and C**). Given the lower
411 amounts of Fbp1 and Fbp2 in adult adipocytes compared to larvae, we confirmed Fbp1 and
412 Fbp2 expression in adult female fat bodies by western blot (**Fig. 3D and E**). Fbp1 is an
413 ecdysone-inducible gene and is cleaved to generate a 64 kDa fragment (Burmester et al.,
414 1999). Fbp1 is further cleaved when reabsorbed by adipocytes to generate a 47 kDa fragment
415 (Burmester et al., 1999). Taking into consideration the eGFP tag (~27 kDa), the multiple bands
416 present in the Fbp1::eGFP western blots are consistent with ecdysone-induced cleavage of
417 Fbp1.
418 To determine whether receptor-mediated adipocyte reabsorption of storage proteins is
419 required for regulation of GSC number, we knocked down *Fbp1* (as well as the other predicted
420 storage protein receptor, *Fbp2*) in adult female adipocytes (**Fig. S6A-C**) and analyzed GSC
421 maintenance. Relative to *Luc* control, knockdown of *Fbp1* or *Fbp2* did not significantly decrease
422 GSC maintenance over time (**Fig. 3F; Fig. S6D**). These results suggest that Fbp1 nor Fbp2 are
423 required in adult female adipocytes for maintaining GSC number.
424
425 ***Fbp1 and Fbp2 are expressed in ovarian follicle cells but are not required for GSC***
426 ***maintenance.***
427 Because Fbp1 and Fbp2 are not required in adult female adipocytes for regulation of
428 GSC number, we hypothesized that Fbp1 or Fbp2 may be required in the ovarian germline or
429 somatic cell populations for storage protein absorption. We therefore assayed ovarian

430 expression of our CRISPR eGFP knock-in lines for expression in the ovary. Lsp1γ::eGFP was
431 not detected in either the germline or the soma of the adult ovary by immunofluorescence or
432 western blot (**Fig. S7A and B**). Interestingly, we did detect Lsp2::eGFP in adult ovaries (**Fig.**
433 **S7C**), and immunofluorescence showed Lsp2::eGFP in the oocyte of egg chambers as early as
434 stage 9 (**Fig. S7D**). This suggests Lsp2 may be synthesized in oocytes or possibly transported
435 to the oocyte from another tissue (e.g., adipocytes) since *Lsp2* transcripts are not detected by
436 single cell sequencing of the ovary (Li et al., 2022; Rust et al., 2020). Notably, both Fbp1::eGFP
437 (**Fig. 4A**) and Fbp2::eGFP (**Fig. 4B**) are detected in the adult ovary by western blot.
438 Immunofluorescence analysis showed that relative to *Oregon-R* control (**Fig. 4C**), Fbp1::eGFP
439 localized to ovarian follicle cells starting in stage 3 egg chambers and decreased expression
440 after stage 5 (**Fig. 4D**). Fbp1::eGFP was also detected in the cytoplasm of nurse cells beginning
441 in stage 7 egg chambers. In contrast, Fbp2::eGFP exclusively localized to follicle cells (**Fig. 4E**),
442 beginning in the germarium and continuing through the remainder of oogenesis. To our
443 knowledge, this is the first reported localization of Lsp2, Fbp1, and Fbp2 in the adult *Drosophila*
444 ovary, suggesting functional roles in adult females.
445 To determine whether Fbp1 or Fbp2 are required in ovarian follicle cells for GSC
446 number, we designed a modified transgenic line of the commonly used follicle cell driver *tj-Gal4*
447 (Sahai-Hernandez and Nystul, 2013). In addition to follicle cell expression, *tj-Gal4* has ectopic
448 expression in the central nervous system, Malpighian tubules, and adipocytes (**Fig. S7E**;
449 (Weaver et al., 2020). To alleviate expression in the brain, we combined the temperature
450 inducible *tj-Gal4 tubGal80^{ts}* driver with *nSyb-Gal80* (to prevent neuronal Gal4 expression
451 independent of temperature), which significantly decreased expression in the brain when
452 females were incubated at 29°C (**Fig. S7F**). Note there is still significant expression in
453 adipocytes; however, because Fbp1 and Fbp2 are not required in adipocytes to regulate GSC
454 number, we reasoned any differences in GSC maintenance would be due primarily to their
455 requirement in follicle cells. However, knockdown of *Fbp1* or *Fbp2* using *tj-Gal4 tubGal80^{ts};*

456 *nSyb-Gal80* did not significantly decrease the number of GSCs over 15 days relative to *Luc*
457 control (**Fig. 4F and G; Fig. S7G and H**). These results suggest that although Fbp1 and Fbp2
458 are expressed in the follicle cells of the ovary, they are not required for GSC maintenance.
459
460 ***Adipocyte-derived amino acid storage proteins do not influence BMP signaling and E-***
461 ***Cadherin levels in GSCs.***
462 GSCs are maintained in the niche primarily through Bone Morphogenic Protein (BMP)
463 signaling from cap cells (Song and Xie, 2002) and by E-Cadherin adhesion to cap cells (Song et
464 al., 2004) to prevent premature differentiation. We asked whether loss of GSCs due to
465 knockdown of *Lsp1*α/β/γ and *Lsp2* in adult adipocytes was mediated by decreased BMP
466 signaling or a reduction in E-Cadherin levels at the niche. To test whether BMP signaling was
467 affected, we measured the nuclear intensity of the Dad::nlsGFP BMP signaling reporter (Ayyaz
468 et al., 2015) when *Lsp1*α/β or *Lsp2* were knocked down specifically in adult female adipocytes
469 after 10 days. Storage protein loss specifically in adult female adipocytes did not have a
470 significant decrease on Dad::nlsGFP levels relative to *Luc* control (**Fig. S8A-C**), suggesting that
471 adipocyte-derived amino acid storage proteins do not regulate BMP signaling. Furthermore,
472 adipocyte-specific loss of storage proteins did not affect E-Cadherin levels in the GSC-niche
473 interface, suggesting a different mechanism is required to maintain GSCs (**Fig. S8D-F**).
474
475 ***Adipocyte-derived storage proteins regulate GSC Target of Rapamycin signaling.***
476 mTOR is a conserved kinase that regulates cell growth and survival downstream of
477 amino acids (Gonzalez and Hall, 2017) and is required in adult female GSCs for stem cell
478 maintenance (LaFever et al., 2010). We hypothesized that adipocyte-derived storage proteins
479 may be transported to the ovary (or some other peripheral tissue) and are catabolized into
480 amino acids to promote TOR signaling. To test this hypothesis, we knocked down *Lsp1*α/β or

481 *Lsp2* specifically in adult female adipocytes using *3.1Lsp2-Gal4*^{ts} and assayed the levels of
482 phosphorylated 4E-BP1 (p4E-BP1), the eukaryotic translation initiation factor 4E binding protein
483 that is phosphorylated by mTOR, which serves as a direct read-out of TOR activity (**Fig. 5A;**
484 (LaFever et al., 2010; Wei et al., 2019). In female GSCs, p4E-BP1 is present during M phase
485 but not G phase (LaFever et al., 2010), which limited the number of GSCs that could be
486 analyzed since mitotic pHH3+ GSCs are only observed in about 5% of the population (Hinnant
487 et al., 2017). Regardless, adipocyte-specific knockdown of amino acid storage proteins
488 significantly decreased p4E-BP1 levels (**Fig. 5B**). Notably, there was no difference in p4E-BP1
489 levels at different mitotic phases (e.g., prometaphase versus metaphase) within an RNAi
490 condition (**Fig. S9A and B**), suggesting the phosphorylation status of 4E-BP1 does not change
491 during early phases of mitosis.

492 To further test whether adipocyte-derived storage proteins regulate mTOR signaling in
493 GSCs, we examined genetic interactions between adipocyte-derived LSPs, *mTOR*, and *Thor*
494 (4E-BP1 in *Drosophila*, a negative regulator of TOR signaling). First, we reasoned that if
495 adipocyte LSPs regulate GSC maintenance though TOR signaling, decreasing the levels of
496 *mTOR* would enhance the GSC loss phenotype, whereas decreasing *Thor* levels would rescue
497 GSC loss. We first combined the *mTOR*$^{\Delta P}$ mutant allele [a P-element insertion that that removes
498 the translation start site and first 902 codons (Zhang et al., 2000)] with *3.1Lsp2*^{ts}. RT-qPCR
499 analysis confirmed a significant reduction in *mTOR* transcripts (**Fig. S9C**). However, the
500 *3.1Lsp2-Gal4* driver in a heterozygous *mTOR*$^{\Delta P}$ background displayed less robust expression
501 compared to control (**Fig. 5C**), preventing further analysis.

502 We next generated a line combining *3.1Lsp2-Gal4*^{ts} with the *Thor*^{2} mutant [an amorphic
503 allele generated from an imprecise P-element excision that removes the entire coding sequence
504 (Bernal and Kimbrell, 2000)]. In this line, *Thor* mRNA was significantly reduced compared to
505 control (**Fig. S9C**) and driver expression was increased (**Fig. 5C**). GSC maintenance was

506 unaffected by one copy of *Thor*^{2} in *Luc* control conditions (**Fig. 5D**, compare control and
507 experimental slopes). By contrast, GSC maintenance due to adipocyte loss of LSPs was
508 significantly rescued by one copy of *Thor*^{2}. Collectively, our results suggest that adipocyte-
509 derived storage proteins act upstream of TOR in GSCs to control GSC maintenance.
510

511 **DISCUSSION**

512 Organism physiology is dependent on modulation of interorgan communication in
513 response to changes in macromolecule levels. Diet-derived amino acids and amino acid
514 sensing are required in multiple cell types to promote stem cell proliferation and self-renewal to
515 maintain tissue homeostasis. In insects, amino acid storage proteins are essential for
516 metamorphosis and organ growth, as well as reproduction. Our results herein show that
517 adipocyte-derived storage proteins are required in adult *Drosophila* females to regulate GSC
518 maintenance to facilitate egg production. Furthermore, our results highlight an uncharacterized
519 requirement for storage proteins in adulthood for female reproduction in *Drosophila*.
520

521 ***Storage proteins are expressed in adult insects.***

522 Although the requirement of storage proteins has been primarily studied for their roles
523 during larval feeding and metamorphosis, storage protein production has also been observed in
524 adult insects (Benes et al., 1990; Martins et al., 2008; Wheeler and Buck, 1995, 1996; Yan et
525 al., 2022). For example, transcripts of the honeybee storage protein *hex 70a* are more abundant
526 in adult female workers compared to males, and there is a significant increase in *hex 70a* fat
527 body transcripts in workers with active ovaries compared to those with inactive ovaries (Martins
528 et al., 2008). Furthermore, *Lsp2* transcripts are detected in the adult *Drosophila* fat body, and
529 the protein accumulates in the hemolymph, albeit at levels significantly decreased compared to
530 larvae (Benes et al., 1990). These results are consistent with our detection of storage proteins
531 (Lsp2::GFP, Fbp1::GFP, and Fbp2::GFP) in adipocytes and the ovary (**Figure 1E and F; Figure**

532 **3D and E; Figure 4A and B; Figure S7A and C**), suggesting undescribed adult specific roles
533 for storage proteins in adult *Drosophila* females.
534 Consistent with our study focused on the roles of storage proteins in adult females, there
535 is evidence that storage protein expression in adult insects is regulated in a sex-specific
536 manner. Synthesis of both *Lsp1* and *Lsp2* occurs in adult females after transplantation of 2nd-
537 instar larval fat bodies, whereas only Lsp1 synthesis can occur after transplantation in males
538 (Butterworth et al., 1979; Jowett and Postlethwait, 1981). In *Bombyx mori*, females accumulate
539 more storage protein compared to males (Tojo et al., 1980), and multiple insects utilize storage
540 proteins to support egg development during adulthood (Wheeler and Buck, 1995, 1996). It has
541 also been shown that females transcribe different hexamerin subunits compared to males
542 (Martins et al., 2010; Tojo et al., 1980; Zakharkin et al., 2001), suggesting a female-specific
543 systemic factor may regulate storage protein synthesis during adulthood. One possible
544 candidate is the steroid hormone ecdysone, considering transcription of *LSPs* and *Fbp1* are
545 ecdysone induced (Burmester et al., 1999). In *Diptera* adults, ecdysone is primarily produced by
546 ovarian follicle cells, accumulating high levels in females but not males (Birnbaum et al., 1984;
547 Bownes et al., 1984; Ono et al., 2006). In *Drosophila* females, increased ecdysone levels and
548 ecdysone signaling in the nervous system promotes female feeding and the nutrient storage
549 required for oogenesis (Sieber and Spradling, 2015). Given that formation of storage granules in
550 larvae corresponds with an increase in ecdysone titers, female-specific activation of ecdysone
551 signaling may provide a feed-forward mechanism for continuous storage protein production to
552 support oogenesis and the developing egg.
553
554 ***Potential roles for storage proteins during oogenesis.***
555 The presence of elevated storage proteins in adult female insects also suggests specific
556 functions during oogenesis. Adult females produce large quantities of vitellogenin to supply
557 developing oocytes with a surplus of amino acids to support embryonic development (Berg et

558 al., 2024). To support developing oocytes, *Lepidoptera* adults rely on larval-derived protein
559 reserves to promote egg production, whereas autogenous insects (such as mosquitos) store
560 glycogen, fat, and protein in the larval fat body that is carried into adulthood (Wheeler and Buck,
561 1996). In contrast, the monarch butterfly produces two methionine-rich hexamerins specifically
562 during adulthood to support egg development (Pan and Telfer, 1996). Other insects have been
563 shown to synthesize and accumulate hexamerins, with storage protein accumulation greater in
564 females that is quickly depleted upon vitellogenesis. For example, virgin queen ants store large
565 quantities of storage proteins that are quickly depleted during the rearing of the first worker ants
566 (Wheeler and Buck, 1995). Although storage proteins have been considered indispensable
567 during *Drosophila* adulthood in some studies, our results are consistent with another report
568 showing other adipocyte-derived factors that are primarily known for their roles in larvae also act
569 as regulators of adult oogenesis (Simmons et al., 2025). Furthermore, we found that
570 Lsp2::eGFP is present in the oocyte of developing egg chambers (**Figure S7D**) and both
571 Fbp1::eGFP and Fbp2::eGFP are present in ovarian follicle cells (**Figure 4D and E**), suggesting
572 additional roles during oogenesis [e.g., possibly mediating the uptake of Lsp2 or additional
573 adipocyte-derived yolk proteins into the oocyte (Berg et al., 2024)] or embryonic development
574 undiscovered by our analysis.
575
576 ***Adipocyte-derived factors are required for oogenesis.***
577 Although present in other tissues, the primary site of hexamerin synthesis is in the insect
578 fat body (Burmester and Scheller, 1997; Haunerland, 1996; Telfer and Kunkel, 1991). The fat
579 body serves as a major endocrine organ in insects (Li et al., 2019) and fat body-specific
580 pathways indirectly influence oogenesis, including GSC maintenance (Armstrong and
581 Drummond-Barbosa, 2018; Armstrong et al., 2014; Matsuoka et al., 2017; Weaver and
582 Drummond-Barbosa, 2018, 2019). For example, adipocyte-secreted collagen IV is required to
583 maintain ovarian GSCs by promoting E-Cadherin mediated adhesion of GSCs to the niche

584 (Weaver and Drummond-Barbosa, 2018). In addition, multiple diet-dependent pathways that
585 regulate amino acid production are altered when adult *Drosophila* females are fed a protein-
586 poor diet (Matsuoka et al., 2017). Furthermore, amino acid sensing in adult female adipocytes
587 influences GSC number in a TOR-independent manner, whereas adipocyte-specific TOR
588 activity influences ovulation (Armstrong et al., 2014). Considering storage protein synthesis in
589 larval adipocytes occurs downstream of TOR (Valzania et al., 2024), it was interesting we did
590 not observe defects in ovulation for when *Lsp1*$\alpha/\beta/\gamma$ or *Lsp2* were knocked down in adipocytes
591 compared to control (0% of ovaries has 2 or more stage 14 embryos per ovariole for all
592 genotypes). Therefore, our results suggest production and secretion of adipocyte-derived
593 storage proteins may occur in a TOR-independent manner [possibly downstream of fat-specific
594 insulin or amino acid response pathways, which also regulate GSC number (Armstrong and
595 Drummond-Barbosa, 2018; Armstrong et al., 2014)]. Furthermore, it is possible that storage
596 proteins act directly downstream of Svp or ecdysone signaling in adult female fat. Interestingly,
597 publicly available data from modENCODE (Consortium, 2012; Roy et al., 2010) shows Svp
598 binding on each storage protein loci in pupae (**Fig. S10**). In contrast, EcR in does not show high
599 occupancy at this stage. Future studies should address whether Svp or EcR bind to regulatory
600 regions of storage proteins to regulate their expression specifically in adult female adipocytes.
601
602 ***Maintenance of GSCs requires activation of amino acid-dependent pathways.***
603 Stem cells and cancer stem cells rapidly proliferate and require increased amino acid
604 metabolism to maintain their self-proliferative and differentiation activities (Gong et al., 2025). In
605 *Drosophila*, larval neuroblasts require diet-derived amino acids to support growth and
606 proliferation (Chell and Brand, 2010). Loss of the amino acid transporter *slimfast* in
607 hematopoietic progenitors causes premature differentiation, resulting in decreased progenitor
608 cell number (Shim et al., 2012). Storage proteins have recently been shown to accumulate in
609 *Drosophila* larval tumors where they are required to promote cancer progression (Valzania et

610 al., 2025). In addition, dietary methionine is required for activation of S-adenosylmethionine to
611 regulate the division rate of intestinal stem cells (Obata et al., 2018). Adult female GSCs directly
612 sense amino acids and activate TOR signaling to control GSC number (LaFever et al., 2010).
613 Our results suggest that adipocyte-derived amino acid storage proteins are required to promote
614 TOR signaling in GSCs (**Figure 5**), suggesting that storage proteins could be trafficked to the
615 ovary where they are catabolized to their amino acid precursors before transportation into
616 GSCs. In larval adipocytes, Fbp1 is required for storage protein reabsorption into the fat prior to
617 metamorphosis (Valzania et al., 2024). However, we did not observe Fbp1::eGFP localization in
618 the GSC niche area suggesting that Fbp1 may not be mediating trafficking of storage proteins
619 into GSCs. It is possible that Fbp1 (or Fbp2) are required in a separate tissue or cell type to
620 catabolize LSPs to regulate GSC maintenance. Single cell RNA sequencing analysis show that
621 *Fbp2* transcripts are present in adult gut enterocytes (Li et al., 2022). Therefore, future studies
622 should systematically knock down *Fbp1* and *Fbp2* in different adult tissues to determine which
623 cell type may be required for LSP absorption to control GSC number. Furthermore, multiple
624 amino acid transporter transcripts are expressed in the ovary (Wright and Armstrong, 2024),
625 and single cell sequencing analysis suggests that multiple transporters are expressed in female
626 GSCs (Li et al., 2022). Future studies should also address the germline requirement for
627 transporters that traffic aromatic amino acids and their relationship with adipocyte-derived
628 storage proteins in regulating TOR signaling and GSC maintenance in the adult female ovary.
629

630 **DATA AVAILABILITY**

631 *Drosophila* strains are available from the Weaver lab upon request. However, any strains
632 that are available from the Bloomington *Drosophila* Stock Center (BDSC) must be obtained
633 through the BDSC. All data generated for this study are included in the main text and figures or
634 in the supplemental file provided.
635

ACKNOWLEDGEMENTS

We thank the Bloomington *Drosophila* Stock Center [National Institutes of Health (NIH) P40OD018537] and the Vienna *Drosophila* Resource Center for *Drosophila* stocks. We are thankful to Flybase (www.flybase.org/), an essential *Drosophila* research resource (NIH 5U41HG000739). The authors would like to thank the Indiana University Light Microscopy Imaging Center (LMIC) for access to microscopy facilities. We are grateful to Deepika Vasudevan and Andrew Zelhof for critical reading of the manuscript. This work was supported by the NIH grants R00GM127605 and R35GM150517 to L.N.W.

FUNDING

This work was supported by the National Institutes of Health (NIH) grants R00GM127605 (L.N.W.) and R35GM150517 (L.N.W).

DECLARATION OF INTERESTS

The authors declare no conflict of interests.

AUTHOR CONTRIBUTIONS

L.N.W. designed experiments, analyzed and interpreted data, and wrote the manuscript. A.B.Z., M.O.H., M.G.A., E.B.G., R.C.E., and L.N.W. performed experiments.

REFERENCES

Akam, M.E., Roberts, D.B., Wolfe, J., 1978. Drosophila hemolymph proteins: purification, characterization, and genetic mapping of larval serum protein 2 in D. melanogaster. Biochem Genet 16, 101-119.

661 Alvarez-Ochoa, E., Froldi, F., Cheng, L.Y., 2021. Interorgan communication in development and
662 cancer. Wiley interdisciplinary reviews. Developmental biology 10, e394.
663
664 Armstrong, A.R., Drummond-Barbosa, D., 2018. Insulin signaling acts in adult adipocytes via
665 GSK-3beta and independently of FOXO to control Drosophila female germline stem cell
666 numbers. Developmental biology 440, 31-39.
667
668 Armstrong, A.R., Laws, K.M., Drummond-Barbosa, D., 2014. Adipocyte amino acid sensing
669 controls adult germline stem cell number via the amino acid response pathway and
670 independently of Target of Rapamycin signaling in Drosophila. Development 141, 4479-4488.
671
672 Arrese, E.L., Soulages, J.L., 2010. Insect fat body: energy, metabolism, and regulation. Annu
673 Rev Entomol 55, 207-225.
674
675 Asha, H., Nagy, I., Kovacs, G., Stetson, D., Ando, I., Dearolf, C.R., 2003. Analysis of Ras-
676 induced overproliferation in Drosophila hemocytes. Genetics 163, 203-215.
677
678 Ayyaz, A., Li, H., Jasper, H., 2015. Hemocytes control stem cell activity in the Drosophila
679 intestine. Nature Cell Biology 17, 736-748.
680
681 Benes, H., Edmondson, R.G., Fink, P., Kejzlarova-Lepesant, J., Lepesant, J.A., Miles, J.P.,
682 Spivey, D.W., 1990. Adult expression of the Drosophila Lsp-2 gene. Developmental biology 142,
683 138-146.
684
685 Berg, C., Sieber, M., Sun, J., 2024. Finishing the egg. Genetics 226.
686

687 Bernal, A., Kimbrell, D.A., 2000. Drosophila Thor participates in host immune defense and
688 connects a translational regulator with innate immunity. Proceedings of the National Academy of
689 Sciences of the United States of America 97, 6019-6024.
690
691 Birnbaum, M.J., Kelly, T.J., Woods, C.W., Imberski, R.B., 1984. Hormonal regulation of ovarian
692 ecdysteroid production in the autogenous mosquito, Aedes atropalpus. Gen Comp Endocrinol
693 56, 9-18.
694
695 Bownes, M., Dübendorfer, A., Smith, T., 1984. Ecdysteroids in adult males and females of
696 Drosophila melanogaster. Journal of insect physiology 30, 823-830.
697
698 Burmester, T., Antoniewski, C., Lepesant, J.A., 1999. Ecdysone-regulation of synthesis and
699 processing of fat body protein 1, the larval serum protein receptor of Drosophila melanogaster.
700 Eur J Biochem 262, 49-55.
701
702 Burmester, T., Scheller, K., 1997. Conservation of hexamerin endocytosis in Diptera. Eur J
703 Biochem 244, 713-720.
704
705 Butterworth, F.M., Tysell, B., Waclawski, I., 1979. The effect of 20-hydroxyecdysone and protein
706 on granule formation in the in vitro cultured fat body of Drosophila. Journal of insect physiology
707 25, 855-860.
708
709 Castillo-Armengol, J., Fajas, L., Lopez-Mejia, I.C., 2019. Inter-organ communication: a
710 gatekeeper for metabolic health. EMBO reports 20.
711

712 Chatterjee, N., Perrimon, N., 2021. What fuels the fly: Energy metabolism in Drosophila and its
713 application to the study of obesity and diabetes. Sci Adv 7.
714
715 Chell, J.M., Brand, A.H., 2010. Nutrition-responsive glia control exit of neural stem cells from
716 quiescence. Cell 143, 1161-1173.
717
718 Chen, H., Liu, C., Cui, S., Xia, Y., Zhang, K., Cheng, H., Peng, J., Yu, X., Li, L., Yu, H., Zhang,
719 J., Zheng, J.S., Zhang, B., 2025. Intermittent fasting triggers interorgan communication to
720 suppress hair follicle regeneration. Cell 188, 157-174 e122.
721
722 Consortium, E.P., 2012. An integrated encyclopedia of DNA elements in the human genome.
723 Nature 489, 57-74.
724
725 Droujinine, I.A., Meyer, A.S., Wang, D., Udeshi, N.D., Hu, Y., Rocco, D., McMahon, J.A., Yang,
726 R., Guo, J., Mu, L., Carey, D.K., Svinkina, T., Zeng, R., Branon, T., Tabatabai, A., Bosch, J.A.,
727 Asara, J.M., Ting, A.Y., Carr, S.A., McMahon, A.P., Perrimon, N., 2021. Proteomics of protein
728 trafficking by in vivo tissue-specific labeling. Nat Commun 12, 2382.
729
730 Droujinine, I.A., Perrimon, N., 2016. Interorgan Communication Pathways in Physiology: Focus
731 on Drosophila. Annu Rev Genet 50, 539-570.
732
733 Drummond-Barbosa, D., 2019. Local and Physiological Control of Germline Stem Cell Lineages
734 in Drosophila melanogaster. Genetics 213, 9-26.
735
736 Drummond-Barbosa, D., Spradling, A.C., 2001. Stem cells and their progeny respond to
737 nutritional changes during Drosophila oogenesis. Developmental biology 231, 265-278.

Fleck, S.A., Biswas, P., DeWitt, E.D., Knuteson, R.L., Eisman, R.C., Nemkov, T., D'Alessandro, A., Tennessen, J.M., Rideout, E., Weaver, L.N., 2024. Auxin exposure disrupts feeding behavior and fatty acid metabolism in adult Drosophila. eLife 12.

Gandara, A.C.P., Drummond-Barbosa, D., 2022. Warm and cold temperatures have distinct germline stem cell lineage effects during Drosophila oogenesis. Development 149.

Gong, Y., Wang, X., Chen, W., Tsai, H.I., Liu, Y., 2025. Cancer stem cells amino acid metabolism: Roles, mechanisms, and intervention strategies. Cell Signal 134, 111903.

Gonzalez, A., Hall, M.N., 2017. Nutrient sensing and TOR signaling in yeast and mammals. The EMBO journal 36, 397-408.

Hales, K.G., Korey, C.A., Larracuente, A.M., Roberts, D.M., 2015. Genetics on the Fly: A Primer on the Drosophila Model System. Genetics 201, 815-842.

Haunerland, N.H., 1996. Insect storage proteins: gene families and receptors. Insect Biochem Mol Biol 26, 755-765.

He, L., Wang, X., Montell, D.J., 2011. Shining light on Drosophila oogenesis: live imaging of egg development. Curr Opin Genet Dev 21, 612-619.

Hinnant, T.D., Alvarez, A.A., Ables, E.T., 2017. Temporal remodeling of the cell cycle accompanies differentiation in the Drosophila germline. Developmental biology 429, 118-131.

764 Hsu, H.J., Drummond-Barbosa, D., 2009. Insulin levels control female germline stem cell
765 maintenance via the niche in Drosophila. Proceedings of the National Academy of Sciences of
766 the United States of America 106, 1117-1121.
767
768 Hsu, H.J., Drummond-Barbosa, D., 2011. Insulin signals control the competence of the
769 Drosophila female germline stem cell niche to respond to Notch ligands. Developmental biology
770 350, 290-300.
771
772 Jowett, T., Postlethwait, J.H., 1981. Hormonal regulation of synthesis of yolk proteins and a
773 larval serum protein (LSP2) in Drosophila. Nature 292, 633-635.
774
775 Katagiri, H., 2023. Inter-organ communication involved in metabolic regulation at the whole-
776 body level. Inflamm Regen 43, 60.
777
778 Kosakamoto, H., Okada, R., Barker, C., Seita, J., Dohmae, N., Imami, K., Obata, F., 2025.
779 Storage Protein-Mediated Translation Control Links Juvenile Diet to Longevity in Drosophila.
780 bioRxiv, 2025.2005.2018.654697.
781
782 LaFever, L., Drummond-Barbosa, D., 2005. Direct control of germline stem cell division and cyst
783 growth by neural insulin in Drosophila. Science 309, 1071-1073.
784
785 LaFever, L., Feoktistov, A., Hsu, H.J., Drummond-Barbosa, D., 2010. Specific roles of Target of
786 rapamycin in the control of stem cells and their progeny in the Drosophila ovary. Development
787 137, 2117-2126.
788

789 Lazareva, A.A., Roman, G., Mattox, W., Hardin, P.E., Dauwalder, B., 2007. A role for the adult
790 fat body in Drosophila male courtship behavior. PLoS genetics 3, e16.
791
792 Li, H., Janssens, J., De Waegeneer, M., Kolluru, S.S., Davie, K., Gardeux, V., Saelens, W.,
793 David, F.P.A., Brbic, M., Spanier, K., Leskovec, J., McLaughlin, C.N., Xie, Q., Jones, R.C.,
794 Brueckner, K., Shim, J., Tattikota, S.G., Schnorrer, F., Rust, K., Nystul, T.G., Carvalho-Santos,
795 Z., Ribeiro, C., Pal, S., Mahadevaraju, S., Przytycka, T.M., Allen, A.M., Goodwin, S.F., Berry,
796 C.W., Fuller, M.T., White-Cooper, H., Matunis, E.L., DiNardo, S., Galenza, A., O'Brien, L.E.,
797 Dow, J.A.T., sign, F.C.A.C.s., Jasper, H., Oliver, B., Perrimon, N., Deplancke, B., Quake, S.R.,
798 Luo, L., Aerts, S., Agarwal, D., Ahmed-Braimah, Y., Arbeitman, M., Ariss, M.M., Augsburger, J.,
799 Ayush, K., Baker, C.C., Banisch, T., Birker, K., Bodmer, R., Bolival, B., Brantley, S.E., Brill, J.A.,
800 Brown, N.C., Buehner, N.A., Cai, X.T., Cardoso-Figueiredo, R., Casares, F., Chang, A.,
801 Clandinin, T.R., Crasta, S., Desplan, C., Detweiler, A.M., Dhakan, D.B., Dona, E., Engert, S.,
802 Floc'hlay, S., George, N., Gonzalez-Segarra, A.J., Groves, A.K., Gumbin, S., Guo, Y., Harris,
803 D.E., Heifetz, Y., Holtz, S.L., Horns, F., Hudry, B., Hung, R.J., Jan, Y.N., Jaszczak, J.S.,
804 Jefferis, G., Karkanias, J., Karr, T.L., Katheder, N.S., Kezos, J., Kim, A.A., Kim, S.K., Kockel, L.,
805 Konstantinides, N., Kornberg, T.B., Krause, H.M., Labott, A.T., Laturney, M., Lehmann, R.,
806 Leinwand, S., Li, J., Li, J.S.S., Li, K., Li, K., Li, L., Li, T., Litovchenko, M., Liu, H.H., Liu, Y., Lu,
807 T.C., Manning, J., Mase, A., Matera-Vatnick, M., Matias, N.R., McDonough-Goldstein, C.E.,
808 McGeever, A., McLachlan, A.D., Moreno-Roman, P., Neff, N., Neville, M., Ngo, S., Nielsen, T.,
809 O'Brien, C.E., Osumi-Sutherland, D., Ozel, M.N., Papatheodorou, I., Petkovic, M., Pilgrim, C.,
810 Pisco, A.O., Reisenman, C., Sanders, E.N., Dos Santos, G., Scott, K., Sherlekar, A., Shiu, P.,
811 Sims, D., Sit, R.V., Slaidina, M., Smith, H.E., Sterne, G., Su, Y.H., Sutton, D., Tamayo, M., Tan,
812 M., Tastekin, I., Treiber, C., Vacek, D., Vogler, G., Waddell, S., Wang, W., Wilson, R.I., Wolfner,
813 M.F., Wong, Y.E., Xie, A., Xu, J., Yamamoto, S., Yan, J., Yao, Z., Yoda, K., Zhu, R., Zinzen,

814 R.P., 2022. Fly Cell Atlas: A single-nucleus transcriptomic atlas of the adult fruit fly. Science
815 375, eabk2432.
816
817 Li, S., Yu, X., Feng, Q., 2019. Fat Body Biology in the Last Decade. Annu Rev Entomol 64, 315-
818 333.
819
820 Liu, C.C., Khan, A., Seban, N., Littlejohn, N., Shah, A., Srinivasan, S., 2024. A homeostatic gut-
821 to-brain insulin antagonist restrains neuronally stimulated fat loss. Nat Commun 15, 6869.
822
823 Ma, T., Matsuoka, S., Drummond-Barbosa, D., 2020. RNAi-based screens uncover a potential
824 new role for the orphan neuropeptide receptor Moody in Drosophila female germline stem cell
825 maintenance. PloS one 15, e0243756.
826
827 Martins, J.R., Nunes, F.M., Cristino, A.S., Simoes, Z.L., Bitondi, M.M., 2010. The four
828 hexamerin genes in the honey bee: structure, molecular evolution and function deduced from
829 expression patterns in queens, workers and drones. BMC Mol Biol 11, 23.
830
831 Martins, J.R., Nunes, F.M., Simoes, Z.L., Bitondi, M.M., 2008. A honeybee storage protein
832 gene, hex 70a, expressed in developing gonads and nutritionally regulated in adult fat body.
833 Journal of insect physiology 54, 867-877.
834
835 Matsuoka, S., Armstrong, A.R., Sampson, L.L., Laws, K.M., Drummond-Barbosa, D., 2017.
836 Adipocyte Metabolic Pathways Regulated by Diet Control the Female Germline Stem Cell
837 Lineage in Drosophila melanogaster. Genetics 206, 953-971.
838

839 Mohr, S.E., 2018. First in fly: Drosophila research and biological discovery. Harvard University
840 Press, United States.
841
842 Morigny, P., Boucher, J., Arner, P., Langin, D., 2021. Lipid and glucose metabolism in white
843 adipocytes: pathways, dysfunction and therapeutics. Nat Rev Endocrinol 17, 276-295.
844
845 Ni, J.Q., Zhou, R., Czech, B., Liu, L.P., Holderbaum, L., Yang-Zhou, D., Shim, H.S., Tao, R.,
846 Handler, D., Karpowicz, P., Binari, R., Booker, M., Brennecke, J., Perkins, L.A., Hannon, G.J.,
847 Perrimon, N., 2011. A genome-scale shRNA resource for transgenic RNAi in Drosophila. Nature
848 methods 8, 405-407.
849
850 Obata, F., Tsuda-Sakurai, K., Yamazaki, T., Nishio, R., Nishimura, K., Kimura, M., Funakoshi,
851 M., Miura, M., 2018. Nutritional Control of Stem Cell Division through S-Adenosylmethionine in
852 Drosophila Intestine. Developmental cell 44, 741-751 e743.
853
854 Ono, H., Rewitz, K.F., Shinoda, T., Itoyama, K., Petryk, A., Rybczynski, R., Jarcho, M., Warren,
855 J.T., Marques, G., Shimell, M.J., Gilbert, L.I., O'Connor, M.B., 2006. Spook and Spookier code
856 for stage-specific components of the ecdysone biosynthetic pathway in Diptera. Developmental
857 biology 298, 555-570.
858
859 Pan, M.L., Telfer, W.H., 1996. Methionine-rich hexamerin and arylphorin as precursor reservoirs
860 for reproduction and metamorphosis in female luna moths. Archives of insect biochemistry and
861 physiology 33, 149-162.
862
863 Ro, J., Harvanek, Z.M., Pletcher, S.D., 2014. FLIC: high-throughput, continuous analysis of
864 feeding behaviors in Drosophila. PloS one 9, e101107.

Roberts, D.B., Turing, J.D., Loughlin, S.A.R., 1991. The advantages that accrue to Drosophila melanogaster possessing larval serum protein 1. Journal of insect physiology 37, 391-400.

Roberts, D.B., Wolfe, J., Akam, M.E., 1977. The developmental profiles of two major haemolymph proteins from Drosophila melanogaster. Journal of insect physiology 23, 871-878.

Roote, J., Prokop, A., 2013. How to design a genetic mating scheme: a basic training package for Drosophila genetics. G3 (Bethesda) 3, 353-358.

Roy, S., Ernst, J., Kharchenko, P.V., Kheradpour, P., Negre, N., Eaton, M.L., Landolin, J.M., Bristow, C.A., Ma, L., Lin, M.F., Washietl, S., Arshinoff, B.I., Ay, F., Meyer, P.E., Robine, N., Washington, N.L., Di Stefano, L., Berezikov, E., Brown, C.D., Candeias, R., Carlson, J.W., Carr, A., Jungreis, I., Marbach, D., Sealfon, R., Tolstorukov, M.Y., Will, S., Alekseyenko, A.A., Artieri, C., Booth, B.W., Brooks, A.N., Dai, Q., Davis, C.A., Duff, M.O., Feng, X., Gorchakov, A.A., Gu, T., Henikoff, J.G., Kapranov, P., Li, R., MacAlpine, H.K., Malone, J., Minoda, A., Nordman, J., Okamura, K., Perry, M., Powell, S.K., Riddle, N.C., Sakai, A., Samsonova, A., Sandler, J.E., Schwartz, Y.B., Sher, N., Spokony, R., Sturgill, D., van Baren, M., Wan, K.H., Yang, L., Yu, C., Feingold, E., Good, P., Guyer, M., Lowdon, R., Ahmad, K., Andrews, J., Berger, B., Brenner, S.E., Brent, M.R., Cherbas, L., Elgin, S.C., Gingeras, T.R., Grossman, R., Hoskins, R.A., Kaufman, T.C., Kent, W., Kuroda, M.I., Orr-Weaver, T., Perrimon, N., Pirrotta, V., Posakony, J.W., Ren, B., Russell, S., Cherbas, P., Graveley, B.R., Lewis, S., Micklem, G., Oliver, B., Park, P.J., Celniker, S.E., Henikoff, S., Karpen, G.H., Lai, E.C., MacAlpine, D.M., Stein, L.D., White, K.P., Kellis, M., 2010. Identification of functional elements and regulatory circuits by Drosophila modENCODE. Science 330, 1787-1797.

891 Rust, K., Byrnes, L.E., Yu, K.S., Park, J.S., Sneddon, J.B., Tward, A.D., Nystul, T.G., 2020. A
892 single-cell atlas and lineage analysis of the adult Drosophila ovary. Nat Commun 11, 5628.
893
894 Sahai-Hernandez, P., Nystul, T.G., 2013. A dynamic population of stromal cells contributes to
895 the follicle stem cell niche in the Drosophila ovary. Development 140, 4490-4498.
896
897 Sakers, A., De Siqueira, M.K., Seale, P., Villanueva, C.J., 2022. Adipose-tissue plasticity in
898 health and disease. Cell 185, 419-446.
899
900 Shim, J., Mukherjee, T., Banerjee, U., 2012. Direct sensing of systemic and nutritional signals
901 by haematopoietic progenitors in Drosophila. Nat Cell Biol 14, 394-400.
902
903 Sieber, M.H., Spradling, A.C., 2015. Steroid Signaling Establishes a Female Metabolic State
904 and Regulates SREBP to Control Oocyte Lipid Accumulation. Current biology : CB 25, 993-
905 1004.
906
907 Simmons, C., Williams, I.H., Bradshaw, T.W., Armstrong, A.R., 2025. Adipocyte-Derived
908 CCHamide-1, Eiger, Growth-Blocking Peptide 3, and Unpaired 2 Regulate Drosophila
909 melanogaster Oogenesis. Biomolecules 15.
910
911 Song, X., Wong, M.D., Kawase, E., Xi, R., Ding, B.C., McCarthy, J.J., Xie, T., 2004. Bmp
912 signals from niche cells directly repress transcription of a differentiation-promoting gene, bag of
913 marbles, in germline stem cells in the Drosophila ovary. Development 131, 1353-1364.
914

915 Song, X., Xie, T., 2002. DE-cadherin-mediated cell adhesion is essential for maintaining somatic
916 stem cells in the Drosophila ovary. Proceedings of the National Academy of Sciences of the
917 United States of America 99, 14813-14818.
918
919 Taylor, S.C., Nadeau, K., Abbasi, M., Lachance, C., Nguyen, M., Fenrich, J., 2019. The Ultimate
920 qPCR Experiment: Producing Publication Quality, Reproducible Data the First Time. Trends
921 Biotechnol 37, 761-774.
922
923 Telfer, W.H., Kunkel, J.G., 1991. The function and evolution of insect storage hexamers. Annu
924 Rev Entomol 36, 205-228.
925
926 Tojo, S., Nagata, M., Kobayashi, M., 1980. Storage proteins in the silkworm, Bombyx mori.
927 Insect Biochemistry 10, 289-303.
928
929 Valzania, L., Alami, A., Leopold, P., 2024. A temporal allocation of amino acid resources
930 ensures fitness and body allometry in Drosophila. Developmental cell 59, 2277-2286 e2276.
931
932 Valzania, L., Blanco-Obregon, D., Alami, A., Léopold, P., 2025. Drosophila storage proteins
933 promote both the rate and the duration of tumor growth. bioRxiv, 2025.2010.2002.680002.
934
935 Weaver, L.N., Drummond-Barbosa, D., 2018. Maintenance of Proper Germline Stem Cell
936 Number Requires Adipocyte Collagen in Adult Drosophila Females. Genetics 209, 1155-1166.
937
938 Weaver, L.N., Drummond-Barbosa, D., 2019. The nuclear receptor seven up functions in
939 adipocytes and oenocytes to control distinct steps of Drosophila oogenesis. Developmental
940 biology 456, 179-189.

941

942 Weaver, L.N., Drummond-Barbosa, D., 2020. The Nuclear Receptor Seven Up Regulates
943 Genes Involved in Immunity and Xenobiotic Response in the Adult Drosophila Female Fat Body.
944 G3 (Bethesda) 10, 4625-4635.

945

946 Weaver, L.N., Ma, T., Drummond-Barbosa, D., 2020. Analysis of Gal4 Expression Patterns in
947 Adult Drosophila Females. G3 (Bethesda) 10, 4147-4158.

948

949 Wei, Y., Bettedi, L., Ting, C.Y., Kim, K., Zhang, Y., Cai, J., Lilly, M.A., 2019. The GATOR
950 complex regulates an essential response to meiotic double-stranded breaks in Drosophila. eLife
951 8.

952

953 Wheeler, D.E., Buck, N.A., 1995. Storage proteins in ants during development and colony
954 founding. Journal of insect physiology 41, 885-894.

955

956 Wheeler, D.E., Buck, N.A., 1996. A role for storage proteins in autogenous reproduction in
957 Aedes atropalpus. Journal of insect physiology 42, 961-966.

958

959 Wolfe, J., Akam, M.E., Roberts, D.B., 1977. Biochemical and immunological studies on larval
960 serum protein 1, the major haemolymph protein of Drosophila melanogaster third-instar larvae.
961 Eur J Biochem 79, 47-53.

962

963 Wright, Y., Armstrong, A.R., 2024. Differential amino acid transporter expression in adult
964 Drosophila melanogaster tissues. MicroPubl Biol 2024.

965

966 Yan, J., Xue, Z., Dong, H., Pang, J., Liu, H., Gong, J., Xia, Q., Hou, Y., 2022. Nutrition regulates
967 the expression of storage proteins in Bombyx mori via insulin-like/FoxO signaling pathway.
968 Insect Biochem Mol Biol 149, 103847.
969
970 Zakharkin, S.O., Headley, V.V., Kumar, N.K., Buck, N.A., Wheeler, D.E., Benes, H., 2001.
971 Female-specific expression of a hexamerin gene in larvae of an autogenous mosquito. Eur J
972 Biochem 268, 5713-5722.
973
974 Zhang, H., Stallock, J.P., Ng, J.C., Reinhard, C., Neufeld, T.P., 2000. Regulation of cellular
975 growth by the Drosophila target of rapamycin dTOR. Genes & development 14, 2712-2724.
976

977 **FIGURE LEGENDS**

978 **Figure 1. Amino acid storage proteins are present in larval and adult female fat tissue.**
979 **(A)** Cartoon schematic of the adult *Drosophila* ovariole showing the anterior germarium and
980 progressively older egg chambers. Each egg chamber consists of germ cells (teal; 15 nurse
981 cells and one oocyte) and somatic follicle cells (gray). **(B)** Germline stem cells (GSCs; dark teal)
982 reside in the germarium and are maintained by a somatic niche that is composed of cap cells
983 (pink). Germline cysts are supported by follicle cells (gray) that facilitate budding of the egg
984 chamber. GSCs are identified by the fusome (yellow), which changes morphology as the
985 differentiated cyst undergoes mitotic divisions with incomplete cytokinesis. **(C)** Quantification of
986 normalized transcript expression (FPKM) for storage protein genes in control and adult fat body
987 *svp* RNAi from (Weaver and Drummond-Barbosa, 2020). Data shown as mean ± SEM from
988 three independent experiments. *P<0.05, **P<0.01, ***P<0.001, ****P<0.0001; Student's *t*-test.
989 **(D)** Abundance of amino acid storage proteins in adult females on a rich versus protein poor diet
990 identified in (Matsuoka et al., 2017). **(E,F)** Western blots from whole adult females or dissected
991 carcasses probed with anti-GFP antibodies to detect Lsp1γ::eGFP (E) or Lsp2::eGFP (F). **(G,H)**

992 Third-instar (G) or adult (H) female adipocytes from *Oregon-R* control and amino acid storage
993 eGFP::fusion CRISPR lines. eGFP (green), amino acid storage protein; α-spectrin (magenta),
994 cell outline; DAPI (blue), nuclei. Scale bar = 25 μm. **(I)** SuperPlot quantifying the number of GFP
995 puncta in *Oregon-R* control, Lsp1γ::eGFP, and Lsp2::eGFP in adult female adipocytes. Data
996 shown as mean ± SEM from four independent samples. *P<0.05, ****P<0.0001; Student's *t*-test.
997
998 **Figure 2. Adult adipocyte-specific knockdown of larval serum proteins decreases GSC**
999 **maintenance.**
1000 **(A,B)** Germaria from *Luc* control (A) and adipocyte-specific *Lsp1α* knockdown (B) after 15 days
1001 of transgene expression. Vasa (green), germ cells; α-spectrin (magenta), fusome; LamC
1002 (magenta), cap cell nuclear lamina; DAPI (blue), nuclei. GSCs are outlined. Scale bar, 10 μm.
1003 **(C,D)** Average number of GSCs over time in *Luc* control females and from adipocyte-specific
1004 *Lsp1α/β* (C) or *Lsp2* (D) knockdown. Data shown as mean ± standard error of the mean (SEM)
1005 from three independent experiments. *P<0.05, **P<0.01, ***P<0.001, ****P<0.0001; two-way
1006 ANOVA with interaction.
1007
1008 **Figure 3. Knockdown *Fbp1* or *Fbp2* in adult female adipocytes does not influence GSC**
1009 **number.**
1010 **(A,B)** Third-instar (A) or adult (B) female adipocytes from *Oregon-R* control and Fat body
1011 protein eGFP::fusion CRISPR lines. eGFP (green), amino acid storage protein; α-spectrin
1012 (magenta), cell outline; DAPI (blue), nuclei. Scale bar = 25 μm. Note that the *Oregon-R* control
1013 is identical to Figure 1G and H as all of the fat samples were collected and analyzed at the
1014 same time and under the same conditions. **(C)** SuperPlot showing quantification of the number
1015 of GFP puncta in *Oregon-R* control, Fbp1::eGFP, and Fbp2::eGFP in adult female adipocytes.
1016 Data shown as mean ± SEM from four independent samples. **P<0.01, ****P<0.0001; Student's

1017 *t*-test. **(D,E)** Western blots from whole adult females or dissected carcasses probed with anti-
1018 GFP antibodies to detect Fbp1::eGFP (D) or Fbp2::eGFP (E). **(F)** Average number of GSCs
1019 over time for adipocyte-specific *Fbp1* or *Fbp2* knockdown compared to *Luc* control. Data shown
1020 as mean ± SEM. n.s., no significant differences; two-way ANOVA with interaction.
1021
1022 **Figure 4. Fbp1 and Fbp2 are expressed in adult ovarian follicle cells, but are not required**
1023 **for GSC maintenance.**
1024 **(A,B)** Western blot analysis from whole adult females and carcasses probed with anti-GFP
1025 antibody to detect Fbp1::eGFP (A) or Fbp2::eGFP (B). **(C-E)** Ovarioles from *Oregon-R* (C),
1026 *Fbp1::eGFP* (D), and *Fbp2::eGFP* (E) adult females. eGFP (green), amino acid storage protein;
1027 α-spectrin (magenta), fusome; LamC (magenta), cap cell nuclear lamina; DAPI (blue), nuclei.
1028 Scale bar = 100 μm. **(F,G)** Average number of GSCs over 15 days from follicle cell knockdown
1029 of *Fbp1* (F) and *Fbp2* (G). Data shown as mean ± SEM from three independent experiments.
1030 n.s., no significant differences; two-way ANOVA with interaction.
1031
1032 **Figure 5. Adipocyte-specific knockdown of storage proteins decreases TOR signaling in**
1033 **GSCs.**
1034 **(A)** Anterior portion of germaria from adipocyte-specific *Luc* control and *Lsp2* knockdown 10
1035 days after transgene induction. Phosphorylated 4E-BP1 (p4E-BP1, green), a direct readout of
1036 mTOR signaling (LaFever et al., 2010; Wei et al., 2019); α-spectrin (magenta), fusome; LamC
1037 (magenta), cap cell nuclear lamina; DAPI (blue), nuclei. Scale bar = 2.5 μm. The dotted lines
1038 outline GSCs. **(B)** SuperPlot of p4E-BP1 intensity per GSC for each genotype. At least 20 GSCs
1039 per genotype were analyzed from three independent experiments. Data shown as mean ± 95%
1040 confidence interval for each genotype. $^{*}P < 0.05$, $^{****}P < 0.0001$; Mann-Whitney *U*-test. **(C)**
1041 Representative images of adult female adipocytes from *3.1Lsp2-Gal4*^{ts}, *mTOR*^{DP}*/+; Lsp2-Gal4*^{ts},

1042 or *Thor*^{2}/+; *Lsp2-Gal4*^{ts} expressing *UAS-2xEGFP*. EGFP (green), Phalloidin (cell membrane;

1043 magenta), DAPI (blue), nuclei. Scale bar = 25 μm. **(D)** Frequencies of germaria containing zero-

1044 or-one, two, three, or four-or-more GSCs at multiple times points of adipocyte-specific RNAi

1045 against *Luc* (control), *Lsp1a*, or *Lsp2* in females carrying one copy of *Thor*^{2} compared to their

1046 wild-type controls. The average number of GSCs per germarium is plotted in dark blue. The

1047 number of germaria analyzed is shown inside the bars. Data shown as mean ± SEM. *$P < 0.05$,

1048 ****$P < 0.0001$; two-way ANOVA with interaction.

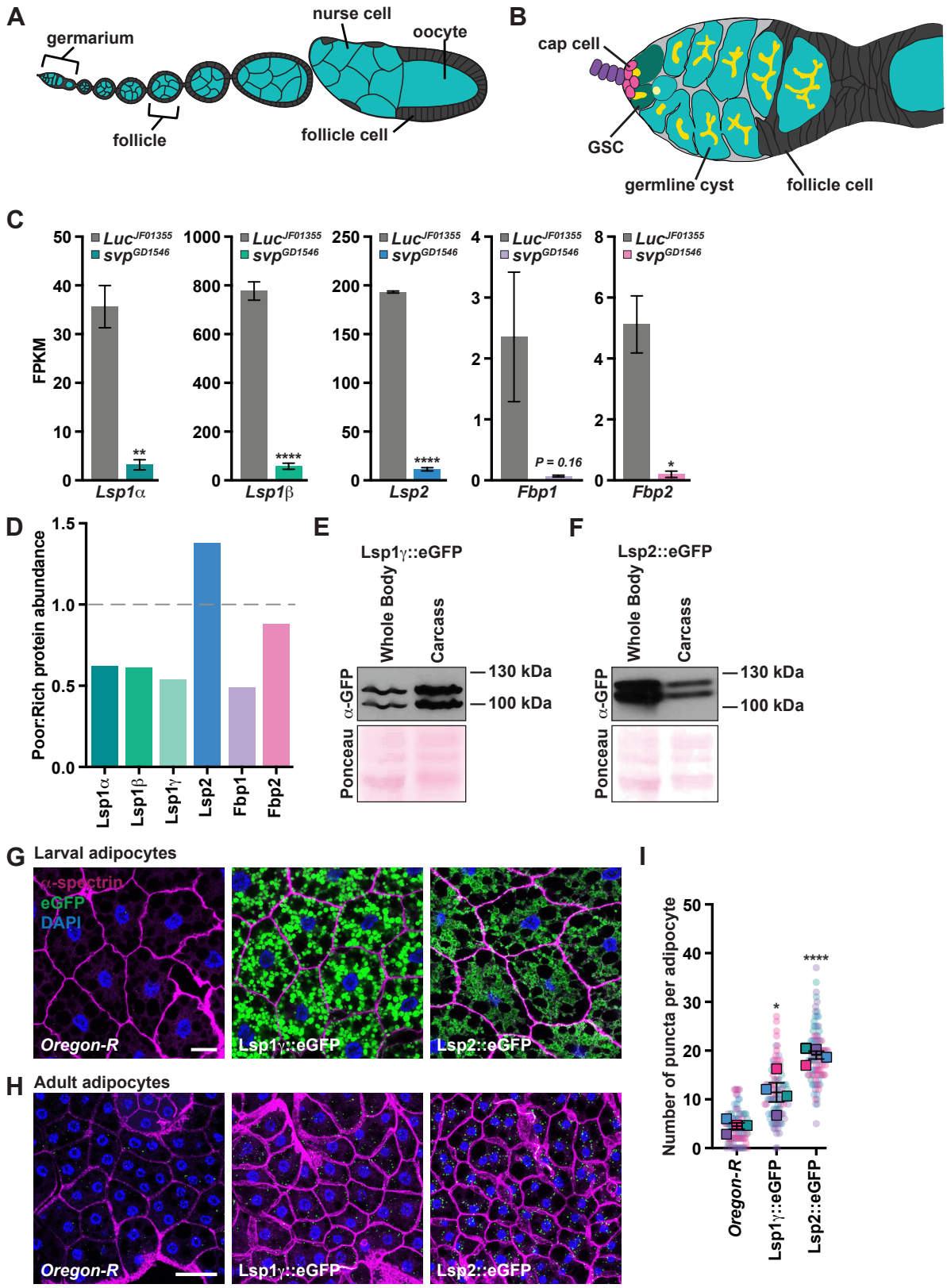

Zike et al.
Figure 1

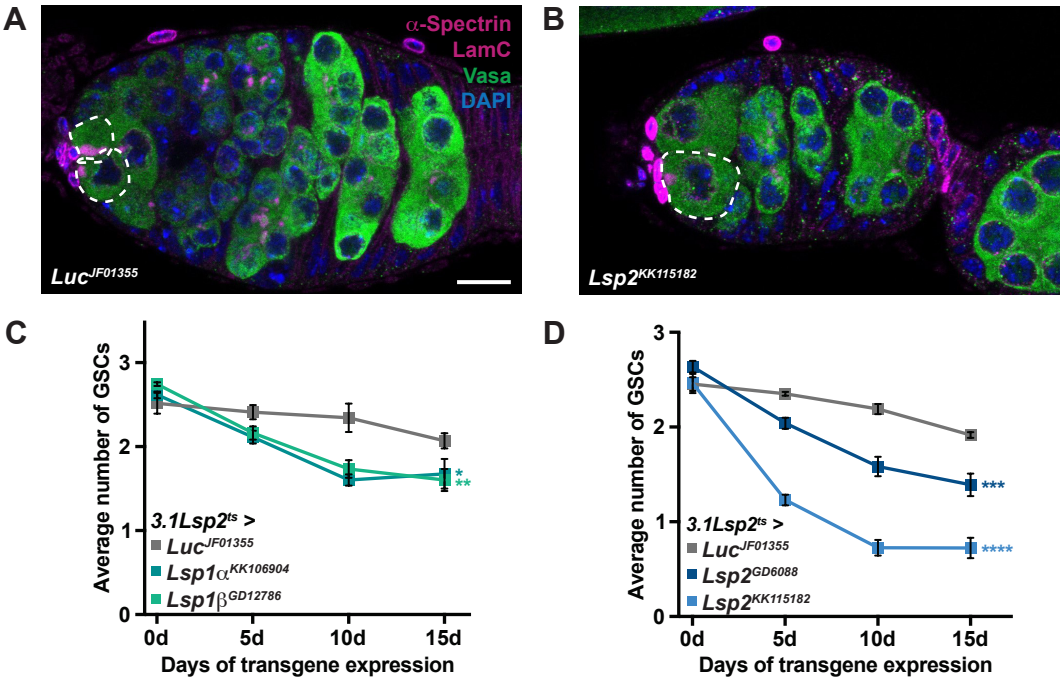

Zike et al.
Figure 2

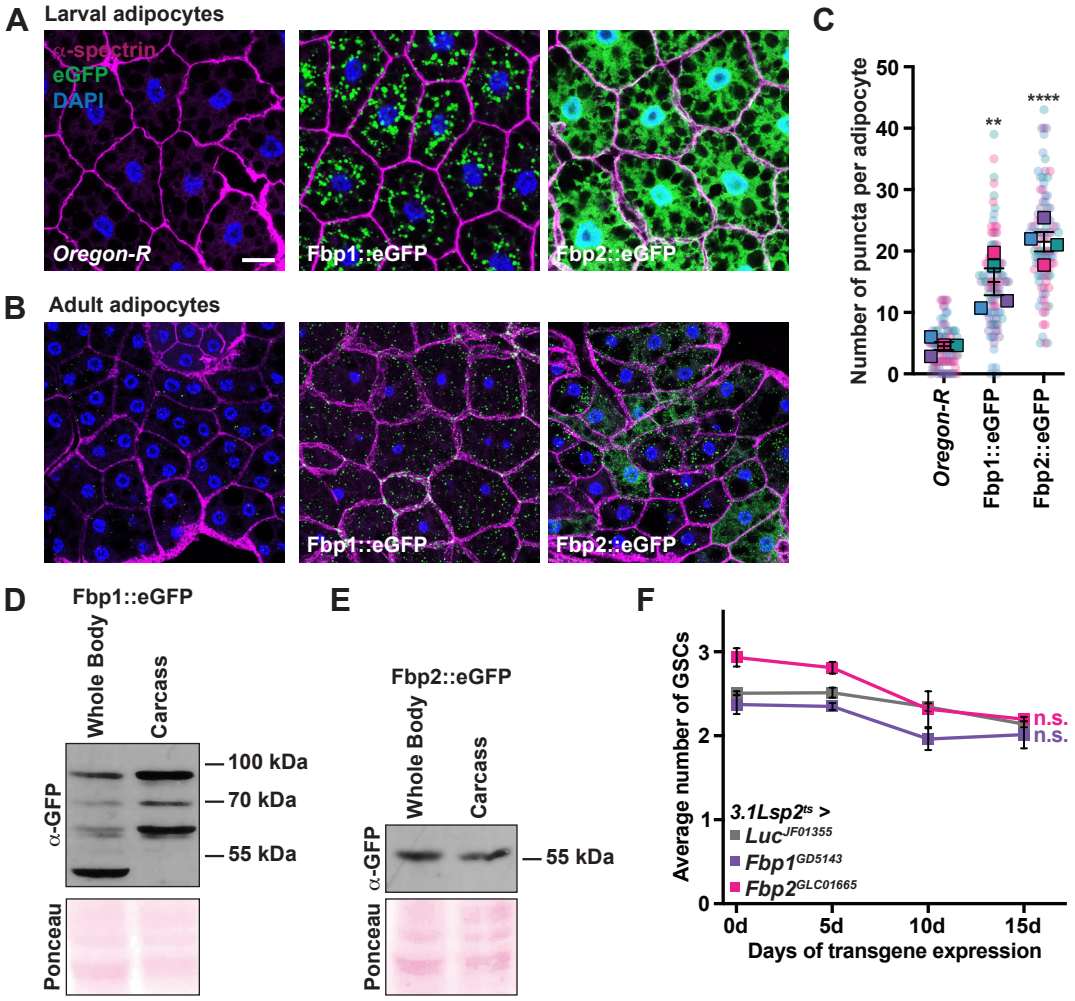

Zike et al.
Figure 3

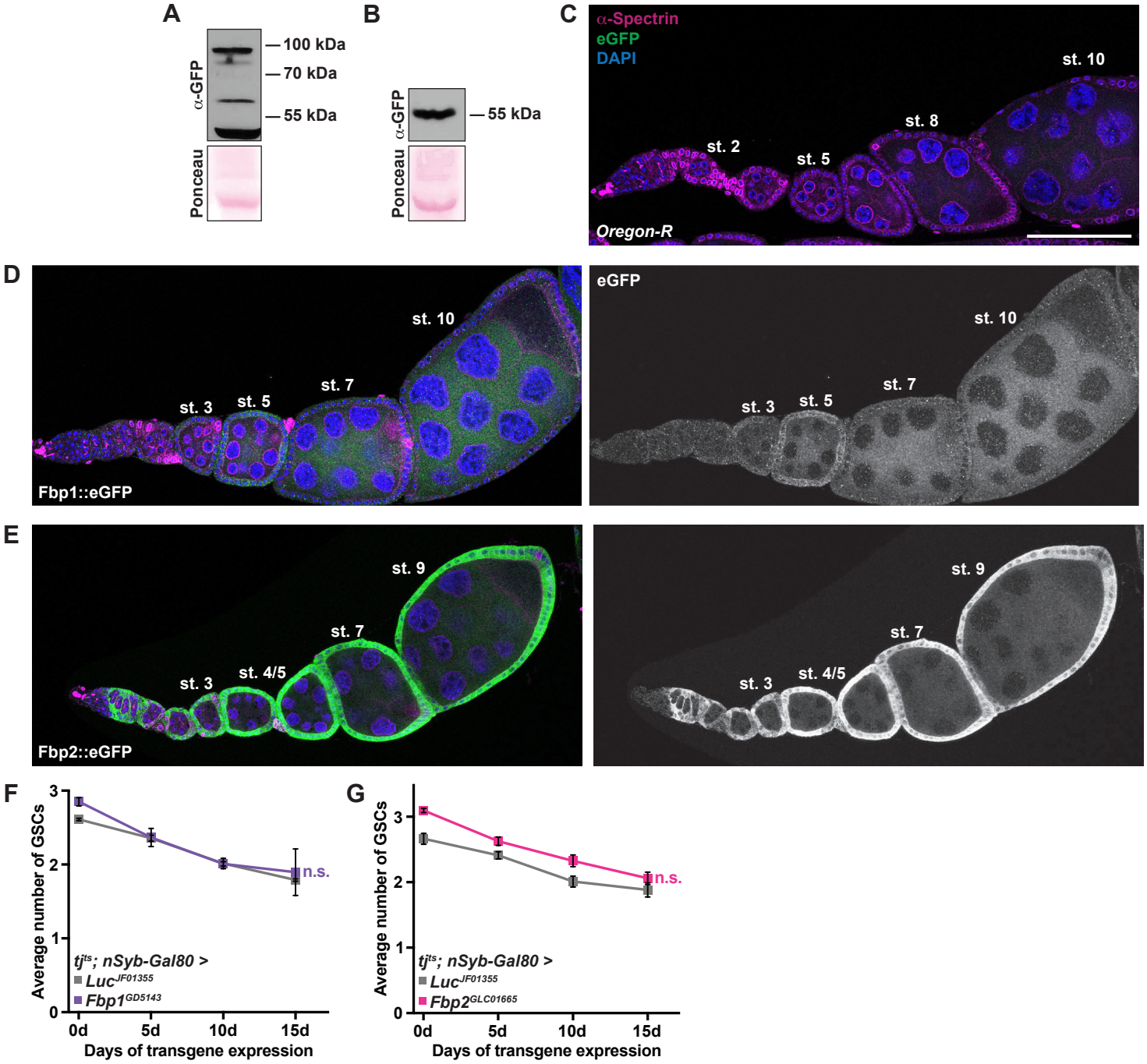

Zike et al.
Figure 4

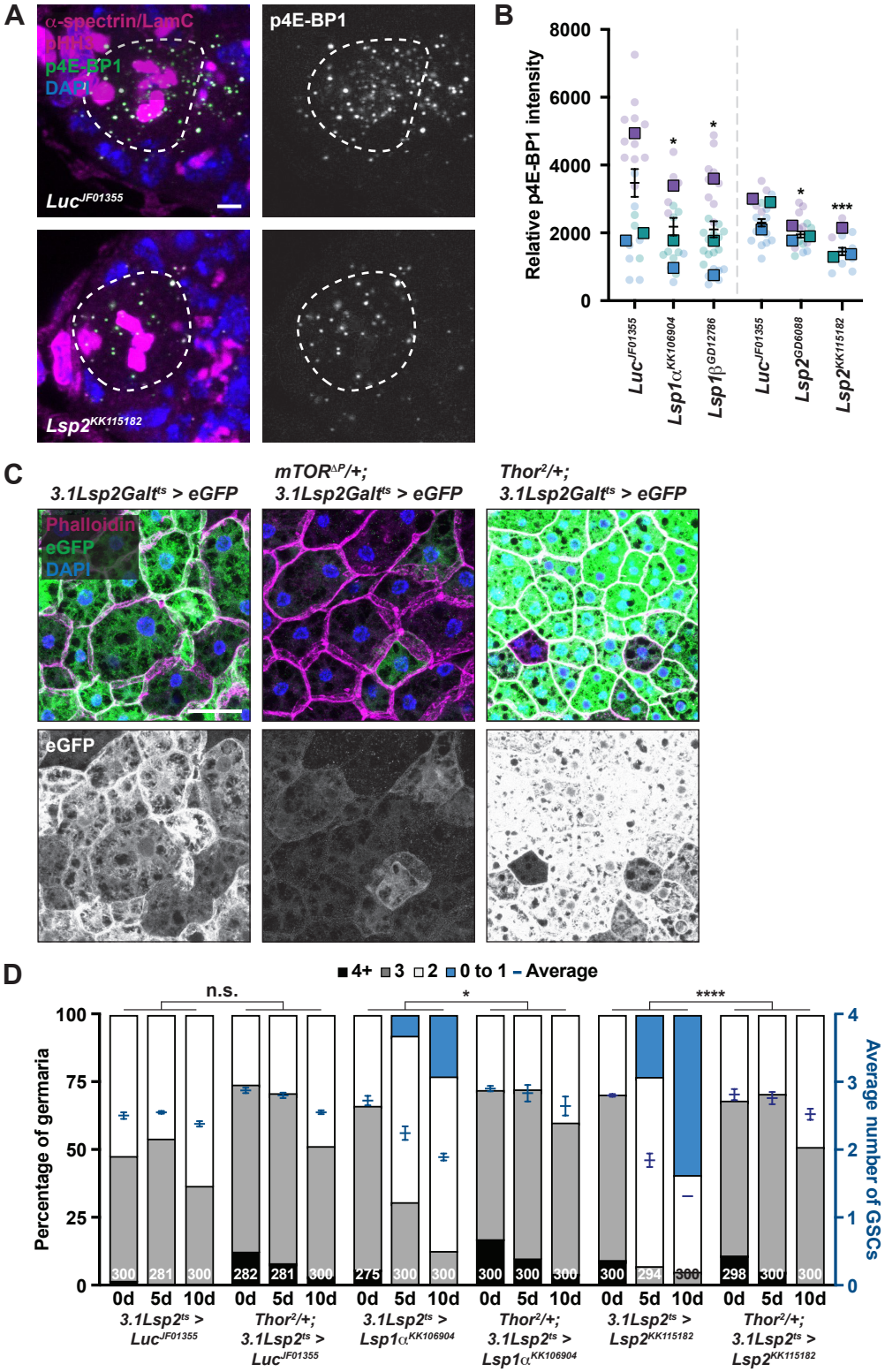

Zike et al.
Figure 5